

# Study of a TPFA scheme for the stochastic Allen-Cahn equation with constraint through numerical experiments

Niklas Sapountzoglou\*      Aleksandra Zimmermann\*

December 22, 2025

## Abstract

This contribution provides numerical experiments for a finite volume scheme for an approximation of the stochastic Allen-Cahn equation with homogeneous Neumann boundary conditions. The approximation is done by a Yosida approximation of the subdifferential operator. The problem is set on a polygonal bounded domain in two or three dimensions. The non-linear character of the projection term induces challenges to implement the scheme. To this end, we provide a splitting method for the finite volume scheme. We show that the splitting method is accurate. The computational error estimates induce that the squared  $L^2$ -error w.r.t. time is of order 1 as long as the noise term is small enough. For larger noise terms the order of convergence w.r.t. time might become worse.

**Keywords:** Stochastic non-linear parabolic equation with constraint  
• Multiplicative Lipschitz noise • Finite volume scheme • Variational approach • Splitting method • Multivoque maximal monotone operator • Differential inclusion • Lagrange multiplier • Numerical experiments.

**Mathematics Subject Classification (2020):** 60H15 • 35K55 • 65M08.

---

<sup>1</sup>TU Clausthal, Institut für Mathematik, Clausthal-Zellerfeld, Germany,  
niklas.sapountzoglou@tu-clausthal.de, aleksandra.zimmermann@tu-clausthal.de

# 1 Introduction

## 1.1 The stochastic Allen-Cahn problem with constraint

Let  $T > 0$  and  $\Lambda$  be a bounded, open, connected, and polygonal set of  $\mathbb{R}^d$ ,  $d \in \{2, 3\}$ , and  $(\Omega, \mathcal{A}, \mathbb{P})$  a probability space endowed with a right-continuous, complete filtration  $(\mathcal{F}_t)_{t \geq 0}$ . We are interested in the study of a TPFA scheme for the time noise-driven Allen-Cahn equation with Neumann boundary conditions, i.e.,

$$\begin{aligned} du + (\psi - \Delta u) dt &= g(u) dW(t) && \text{in } \Omega \times (0, T) \times \Lambda; \\ u(0, \cdot) &= u_0, && \text{in } \Omega \times \Lambda; \\ \nabla u \cdot \mathbf{n} &= 0, && \text{on } \Omega \times (0, T) \times \partial\Lambda; \end{aligned} \tag{1}$$

where  $(W(t))_{t \geq 0}$  is a standard, one-dimensional Brownian motion with respect to  $(\mathcal{F}_t)_{t \geq 0}$  on  $(\Omega, \mathcal{A}, \mathbb{P})$ ,  $\mathbf{n}$  denotes the unit normal vector to  $\partial\Lambda$  outward to  $\Lambda$  and  $\psi \in \partial I_{[0,1]}(u)$ . In this case, we define

$$I_{[0,1]}(r) = \begin{cases} 0 & \text{if } r \in [0, 1] \\ +\infty & \text{else} \end{cases}$$

and the set-valued mapping  $\partial I_{[0,1]} : [0, 1] \rightarrow \mathcal{P}(\mathbb{R})$  is defined by

$$\partial I_{[0,1]}(r) = \begin{cases} \{0\} & \text{if } r \in (0, 1) \\ (-\infty, 0] & \text{if } r = 0 \\ [0, \infty) & \text{if } r = 1. \end{cases} \tag{2}$$

We consider the following assumptions on the data:

- The initial datum  $u_0 \in L^2(\Omega; L^2(\Lambda))$  is  $\mathcal{F}_0$ -measurable and verifies  $0 \leq u_0(\omega, x) \leq 1$ , for almost all  $(\omega, x) \in \Omega \times \Lambda$ .
- The diffusion coefficient  $g : \mathbb{R} \rightarrow \mathbb{R}$  is a  $L_g$ -Lipschitz-continuous function (with  $L_g \geq 0$ ), such that  $\text{supp } g \subset [0, 1]$ .

From the results of [BBBLV17] it is well known, that there exists a unique solution to (1) in the following sense:

**Definition 1.1.** *Any pair of predictable stochastic processes  $(u, \psi)$  with  $u, \psi \in L^2((\Omega \times (0, T); L^2(\Lambda)))$  such that*

$$u \in L^2(\Omega; \mathcal{C}([0, T]; L^2(\Lambda))) \cap L^2(\Omega \times (0, T); H^1(\Lambda)),$$

is a solution to Problem (1) if  $0 \leq u \leq 1$  and  $\psi \in \partial I_{[0,1]}(u)$  almost everywhere in  $\Omega \times (0, T) \times \Lambda$  and if  $(u, \psi)$  satisfies the equation

$$u(t) - u_0 + \int_0^t (\psi(s) - \Delta u(s)) \, ds + \int_0^t g(u(s)) \, dW(s), \quad (3)$$

for all  $t \in [0, T]$  in  $L^2(\Lambda)$ ,  $\mathbb{P}$ -a.s in  $\Omega$ , where  $\Delta$  denotes the Laplace operator on  $H^1(\Lambda)$  associated with the weak Neumann boundary condition.

## 1.2 State of the art

The study of numerical schemes for stochastic partial differential equations (SPDEs) has been a very active subject in recent decades and for this reason, an extensive literature on this topic is available. We refer the interested reader to [ACQS20, DP09, OPW20] for a general overview and to the references therein. Concerning the numerical analysis of variational solutions, in the past the use of finite-element methods has been favored and extensively employed (see, e.g., [BBNP14, BHL21] for a detailed exposition of existing papers). In recent years, there has been increasing interest in numerical approximations which preserve the specific structure of the underlying equations. In this way, important physical properties of the underlying model are implemented at the numerical level, and the robustness and the stability of numerical methods are improved. As pointed out in [D14], among the numerous families of numerical methods, e.g., finite difference, finite element, discontinuous Galerkin, Gradient Discretization Method (GDM), finite-volume methods (FVM) are very well-suited for applications in which the conservation of quantities is important. For finite-volume methods, balance and local conservativity are the leading principles in the construction of numerical fluxes. The Two Point Flux Approximation (TPFA) scheme is a cell-centered finite-volume method which is particularly cheap to implement, since its matrices are very sparse. In the last decade, there has been growing interest in the use of finite-volume methods for the spatial discretization of SPDEs. First, monotone schemes have been derived for the approximation of hyperbolic problems perturbed by multiplicative noise, known as stochastic first order scalar conservation laws in the literature, see, e.g., [BCG162, BCG161, BCC20, BCG17]. More recently, the convergence analysis of a numerical scheme of Euler-Maruyama type with respect to time and of TPFA-type with respect to space for a stochastic heat equation with multiplicative Lipschitz noise has been studied in [BNSZ22]. In this contribution, convergence of approximate solutions was proved by adapting the stochastic compactness method based on Skorokhod's representation theorem. In [BNSZ23, BSZ25], these results have been extended to more general

stochastic PDEs of diffusion-convection type where the convective term is given by a first-order divergence type operator. At the same time, the authors avoided the use of the stochastic compactness argument. In [SZ25], explicit error bounds for the numerical scheme in [BNSZ22] have been developed and complemented with computational experiments. Finally, in [BSVZ25], the methods developed in [BNSZ22] and [BSZ25] have been applied to a stochastic Allen–Cahn problem with constraint. The idea of stochastic Allen–Cahn equations with constraint as considered in [BBBLV17] is to describe the evolution of the damage over time at a solid interface of a composite material by the stochastic differential inclusion

$$du - \Delta u \, dt + \partial I_{[0,1]}(u) \, dt \ni (u) \, dW + (\beta(u) + f) \, dt \quad (4)$$

on a bounded domain of  $\mathbb{R}^d$ , and subject to homogeneous Neumann boundary conditions, where  $\partial I_{[0,1]}$  is defined according to (2). More precisely, our solution  $u$  represents the local proportion of intact bonds within the considered material: It is then a quantity between 0 and 1. The case  $u = 0$  is corresponding to a totally damaged material, the case  $u = 1$  to a material without damage. The physical constraint on the solution  $u$  is ensured by the presence of a multivalued maximal monotone operator. The addition of a stochastic perturbation to this Allen–Cahn model is motivated by the consideration of changes at the microscopic scale of the material structure such as the formation of cavities during damage, the random distribution of micro-cracks and external forces. In [BSVZ25] a finite-volume scheme for the stochastic Allen–Cahn problem with constraint (4) is proposed in the case of a polygonal domain and for the space dimensions  $d = 2$  or  $d = 3$ . Moreover, the convergence of the scheme towards the variational solution is studied. The main feature of the proposed scheme is the approximation of the set-valued constraint by its Yosida approximation. In this way, an additional parameter enters the discrete equation and the passage to the limit is performed simultaneously with the time, space and the regularization parameter. The authors show the convergence of the proposed Euler–Maruyama–TPFA scheme under a coupling condition of the time parameter and the parameter related to the Yosida approximation of the set-valued constraint.

### 1.3 Discretization framework and notation

In the following, we introduce some general notation and recall important definitions related to temporal and spatial discretizations. Let us mention that they are the same as in previous papers [BNSZ22, BNSZ23, BSZ25, SZ25], but we repeat them for the convenience of the reader.

### 1.3.1 General notation

- The integral over  $\Omega$  with respect to the probability measure  $\mathbb{P}$  is denoted by  $\mathbb{E}[\cdot]$ , and is called the expectation.
- For any  $x, y$  in  $\mathbb{R}^d$ , the euclidean norm of  $x$  is denoted by  $|x|$ , and the associated scalar product of  $x$  and  $y$  by  $x \cdot y$ .
- The  $d$ -dimensional Lebesgue measure of  $\Lambda$  is denoted by  $|\Lambda|$ , by overusing the euclidean norm notation.

### 1.3.2 Uniform time step and admissible finite-volume meshes

According to the TPFA scheme proposed in [BSVZ25], we introduce the following temporal and spatial discretizations: The temporal one is achieved using a uniform subdivision: setting  $N \in \mathbb{N}$ , the fixed time step is defined by  $\Delta t = \frac{T}{N}$  and the interval  $[0, T]$  is decomposed in  $0 = t_0 < t_1 < \dots < t_N = T$  equidistantly with  $t_n = n\Delta t$  for all  $n \in \{0, \dots, N - 1\}$ . For the spatial one, following [EGH00, Definition 9.1], we consider admissible finite-volume meshes as defined hereafter:

**Definition 1.2.** (*Admissible finite-volume mesh*) *An admissible finite-volume mesh of  $\Lambda$ , denoted by  $\mathcal{T}$ , is given by a family of “control volumes”, which are open polygonal convex subsets of  $\Lambda$ , a family of subsets of  $\overline{\Lambda}$  contained in hyperplanes of  $\mathbb{R}^d$ , denoted by  $\mathcal{E}$  (these are the edges for  $d = 2$  or sides for  $d = 3$  of the control volumes), with strictly positive  $(d - 1)$ -dimensional Lebesgue measure, and a family of points of  $\Lambda$  denoted by  $\mathcal{P}$  satisfying the following properties<sup>1</sup>*

- $\overline{\Lambda} = \bigcup_{K \in \mathcal{T}} \overline{K}$ .
- For any  $K \in \mathcal{T}$ , there exists a subset  $\mathcal{E}^K$  of  $\mathcal{E}$  such that  $\partial K = \overline{K} \setminus K = \bigcup_{\sigma \in \mathcal{E}^K} \overline{\sigma}$  and  $\mathcal{E} = \bigcup_{K \in \mathcal{T}} \mathcal{E}^K$ .  $\mathcal{E}^K$  is called the set of edges of  $K$  for  $d = 2$  and sides for  $d = 3$ , respectively.
- For any  $K, L \in \mathcal{T}$ , with  $K \neq L$  then either the  $(d - 1)$  Lebesgue measure of  $\overline{K} \cap \overline{L}$  is 0 or  $\overline{K} \cap \overline{L} = \overline{\sigma}$  for some  $\sigma \in \mathcal{E}$ , which will then be denoted by  $K|L$  or  $L|K$ .
- The family  $\mathcal{P} = (x_K)_{K \in \mathcal{T}}$  is such that  $x_K \in \overline{K}$  for all  $K \in \mathcal{T}$  and, if  $K, L \in \mathcal{T}$  are two neighboring control volumes, it is assumed that  $x_K \neq x_L$ , and that the straight line between  $x_K$  and  $x_L$  is orthogonal to  $\sigma = K|L$ .

---

<sup>1</sup>In fact, we shall denote, somewhat incorrectly, by  $\mathcal{T}$  the family of control volumes.

- For any  $\sigma \in \mathcal{E}$  such that  $\sigma \subset \partial\Lambda$ , let  $K$  be the control volume such that  $\sigma \in \mathcal{E}^K$ . If  $x_K \notin \sigma$ , the straight line going through  $x_K$  and orthogonal to  $\sigma$  has a nonempty intersection with  $\sigma$ .

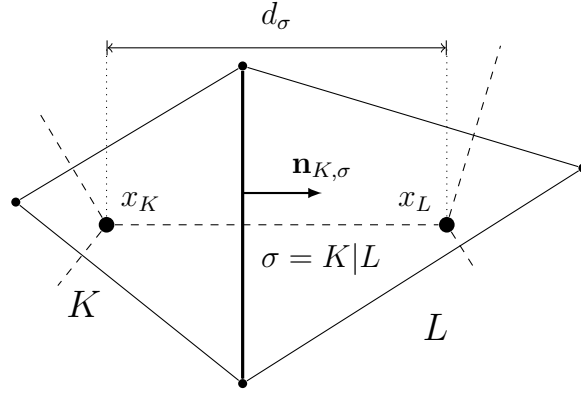


Figure 1: Two neighboring control volumes  $K, L \in \mathcal{T}$  with interface  $\sigma = K|L$  in  $\mathbb{R}^2$

For a given admissible finite-volume mesh  $\mathcal{T}$  of  $\Lambda$ , the following associated notations will be used in the rest of the paper.

### Notations.

- The mesh size is denoted by  $h = \text{size}(\mathcal{T}) = \sup\{\text{diam}(K) : K \in \mathcal{T}\}$ .
- The number of control volumes  $K \in \mathcal{T}$  is denoted by  $d_h \in \mathbb{N}$ , where  $h = \text{size}(\mathcal{T})$ .
- The sets of interior and exterior interfaces are respectively denoted by  $\mathcal{E}_{\text{int}} := \{\sigma \in \mathcal{E} : \sigma \not\subseteq \partial\Lambda\}$  and  $\mathcal{E}_{\text{ext}} := \{\sigma \in \mathcal{E} : \sigma \subseteq \partial\Lambda\}$ . Moreover we set  $\mathcal{E}_{\text{int}}^K := \mathcal{E}^K \cap \mathcal{E}_{\text{int}}$  for any  $K \in \mathcal{T}$ .
- For any  $K \in \mathcal{T}$ , the  $d$ -dimensional Lebesgue measure of  $K$  is denoted by  $m_K$ .
- For any  $K \in \mathcal{T}$ , the unit normal vector to  $\partial K$  outward to  $K$  is denoted by  $\mathbf{n}_K$ .

- For any  $K \in \mathcal{T}$  and any  $\sigma \in \mathcal{E}^K$ , the unit vector on  $\sigma$  pointing out of  $K$  is denoted by  $\mathbf{n}_{K,\sigma}$ .
- For any  $\sigma \in \mathcal{E}_{\text{int}}$ , the  $(d-1)$ -dimensional Lebesgue measure of  $\sigma$  is denoted by  $m_\sigma$ .
- For any neighboring control volumes  $K, L \in \mathcal{T}$ , the euclidean distance between  $x_K$  and  $x_L$  is denoted by  $d_{K|L}$ .
- The maximum of edges incident to any vertex of the mesh is denoted by  $\mathcal{N}$ .
- For any  $K \in \mathcal{T}$  and any  $\sigma \in \mathcal{E}^K$ , the Euclidean distance between  $x_K$  and  $\sigma$  is denoted by  $d(x_K, \sigma)$  and we assume that there exists  $\xi > 0$  such that  $\xi h \leq d(x_K, \sigma)$  for all  $K \in \mathcal{T}$ .

## 1.4 Aim of this study

From the point of view of applications, some questions remain open in [BSVZ25]. The multivalued term in (1) ensures that, for initial data with values in  $[0, 1]$ , the values of the solution  $u$  stay in  $[0, 1]$ . For the sake of structure preservation, it would be desirable that the numerical approximations given by the scheme proposed in [BSVZ25] also take values in  $[0, 1]$ . Secondly, to provide enough regularity on the approximate solutions and to obtain the necessary a-priori estimates, our scheme must be time implicit in the Yosida approximation. Consequently, an approximation procedure is needed to solve the resulting nonlinear equations numerically. Since the Yosida approximations are a sequence of piecewise linear functions with only Lipschitz regularity which is depending on the discretization parameter, this choice is delicate. In this contribution, we address these questions and provide numerical simulations for the scheme developed in [BSVZ25] in the case  $\beta \equiv 0$  and  $f \equiv 0$ . More precisely, we recall the following family of SPDEs depending on a parameter  $\varepsilon > 0$ :

$$\begin{aligned} du_\varepsilon + (\psi_\varepsilon(u_\varepsilon) - \Delta u_\varepsilon) dt &= g(u_\varepsilon) dW(t), & \text{in } \Omega \times (0, T) \times \Lambda; \\ u_\varepsilon(0, \cdot) &= u_0, & \text{in } \Omega \times \Lambda; \\ \nabla u_\varepsilon \cdot \mathbf{n} &= 0, & \text{on } \Omega \times (0, T) \times \partial\Lambda; \end{aligned} \tag{5}$$

where  $\psi_\varepsilon : \mathbb{R} \rightarrow \mathbb{R}$  denotes the Moreau-Yosida approximation of  $\partial I_{[0,1]}$  (see, *e.g.*, [Bar76, Bre73]), defined for all  $v \in \mathbb{R}$  by

$$\psi_\varepsilon(v) = -\frac{(v)^-}{\epsilon} + \frac{(v-1)^+}{\epsilon} = \begin{cases} \frac{v}{\epsilon} & \text{if } v \leq 0 \\ 0 & \text{if } v \in [0, 1] \\ \frac{v-1}{\epsilon} & \text{if } v \geq 1. \end{cases} \tag{6}$$

Taking (5) as a starting point, the following Euler-Maruyama-TPFA-scheme has been proposed in [BSVZ25]:

For a  $\mathcal{F}_0$ -measurable random element  $u_0 \in L^2(\Omega; L^2(\Lambda))$  we define  $\mathbb{P}$ -a.s. in  $\Omega$  its piecewise constant spatial discretization  $u_h^0 = \sum_{K \in \mathcal{T}} u_K^0 \mathbf{1}_K$ , where

$$u_K^0 = \frac{1}{m_K} \int_K u_0(x) dx, \quad \forall K \in \mathcal{T}_h.$$

Now, for any  $n \in \{0, \dots, N-1\}$  and fixed  $\varepsilon > 0$ , assuming the random vector  $u_h^n \equiv (u_K^n)_{K \in \mathcal{T}} \in \mathbb{R}^{d_h}$  to be given, the random vector  $u_h^{n+1} \equiv (u_K^{n+1})_{K \in \mathcal{T}} \in \mathbb{R}^{d_h}$  is defined to be the solution of the following equations:

$$\begin{aligned} & \frac{m_K}{\Delta t} (u_K^{n+1} - u_K^n) + \sum_{\sigma=K|L \in \mathcal{E}_{\text{int}} \cap \mathcal{E}_K} \frac{m_\sigma}{d_{K|L}} (u_K^{n+1} - u_L^{n+1}) + m_K \psi_\varepsilon(u_K^{n+1}) \\ &= \frac{m_K}{\Delta t} g(u_K^n) \Delta_n W \end{aligned} \tag{7}$$

for each  $K \in \mathcal{T}$ ,  $\mathbb{P}$ -a.s in  $\Omega$ , where  $\Delta_n W := W(t_n) - W(t_{n-1})$  denotes the increments of the Brownian motion between  $t_{n+1}$  and  $t_n$ . The following results are known:

**Proposition 1.3.** [BSVZ25, Proposition 3.2] *Let  $\mathcal{T}$  be an admissible finite-volume mesh of  $\Lambda$  in the sense of Definition 1.2 with a mesh size  $h$ . Moreover, let an initial  $\mathcal{F}_0$ -measurable random vector  $u_h^0 \equiv (u_K^0)_{K \in \mathcal{T}} \in \mathbb{R}^{d_h}$ ,  $N \in \mathbb{N}$ , and  $\varepsilon > 0$  be given. Then, there exists a unique solution  $(u_h^n)_{1 \leq n \leq N} \in (\mathbb{R}^{d_h})^N$  to (7). Moreover, for any  $n \in \{0, \dots, N\}$ ,  $u_h^n$  is a  $\mathcal{F}_{t_n}$ -measurable random vector.*

**Theorem 1.4.** [BSVZ25, Theorem 1.5] *Let  $(u, \psi)$  be the unique solution of Problem (1) in the sense of Definition 1.1. Let  $(\mathcal{T}_m)_{m \in \mathbb{N}}$  be a sequence of admissible finite-volume meshes of  $\Lambda$  in the sense of Definition 1.2 such that the sequence of their mesh sizes  $(h_m)_{m \in \mathbb{N}}$  tends to 0. Let  $(N_m)_{m \in \mathbb{N}} \subset \mathbb{N}$  be a sequence which tends to infinity and let  $(\epsilon_m)_{m \in \mathbb{N}}$  be a sequence of positive real numbers such that  $\lim_{m \rightarrow +\infty} \epsilon_m = 0$ . For  $m \in \mathbb{N}$ , let  $u_{h_m, N_m}$  be the piecewise constant function induced by the solutions of (7) according to Proposition 1.3. If there exists  $\theta > 0$  such that, for any  $m \in \mathbb{N}$ ,  $\frac{T}{N_m} = \mathcal{O}((\epsilon_m)^{2+\theta})$ , then the sequence  $(u_{h_m, N_m})_{m \in \mathbb{N}}$  converges to  $u$  and the sequence  $(\psi_{\epsilon_m}(u_{h_m, N_m}))_{m \in \mathbb{N}}$  converges to  $\psi$ , strongly in  $L^2(\Omega; L^2(0, T; L^2(\Lambda)))$ . Moreover, the convergence of  $(u_{h_m, N_m})_{m \in \mathbb{N}}$  towards  $u$  also holds strongly in  $L^p(0, T; L^2(\Omega; L^2(\Lambda)))$  for any finite  $p \geq 1$ .*

Our aim is to study the properties of the scheme (7) through numerical experiments. Besides the questions mentioned above, we provide and discuss

numerical convergence rates with respect to the time step size for (7). In Section 2, we will introduce a splitting method to implement the nonlinear term coming from the Yosida approximation into the scheme and study its convergence. In Section 3 we provide numerical experiments which are relevant for the study of the properties of (7) and provide an interpretation of our results.

## 2 Splitting method

In this section we explain the splitting method we use in Section 3.3 in the cases  $\beta \equiv 0$  and  $f \equiv 0$ . For a vector  $w = (w_K)_{K \in \mathcal{T}} \in \mathbb{R}^{\tilde{d}}$  and any function  $\phi : \mathbb{R} \rightarrow \mathbb{R}$  we will denote  $\phi(w) := (\phi(w_K))_{K \in \mathcal{T}}$  and in this way we may consider  $\psi_\varepsilon$  as a non-linear function from  $\mathbb{R}^{\tilde{d}}$  to  $\mathbb{R}^{\tilde{d}}$ . Let  $u^{n-1} = (u_K^{n-1})_{K \in \mathcal{T}} \in \mathbb{R}^{\tilde{d}}$  be the solution of the FVS after  $n-1$  time steps. Then, the solution  $u^n = (u_K^n)_{K \in \mathcal{T}} \in \mathbb{R}^{\tilde{d}}$  after  $n$  time steps is given by the equation

$$(M + \tau A)u^n + \tau M\psi_\varepsilon(u^n) = M(u^{n-1} + g(u^{n-1})\Delta_n W), \quad (8)$$

where  $M = \text{diag}((m_K)_{K \in \mathcal{T}})$  and  $A = (a_{K,L})_{K,L \in \mathcal{T}} \in \mathbb{R}^{\tilde{d} \times \tilde{d}}$  is a sparse matrix such that

$$\begin{cases} a_{K,K} = \sum_{\sigma \in \mathcal{E}_{int}^K} \frac{m_\sigma}{d_\sigma}, & K \in \mathcal{T} \\ a_{K,L} = -\frac{m_\sigma}{d_\sigma}, & K \in \mathcal{T}, L \in \mathcal{N}(K), \sigma = K|L \\ a_{K,L} = 0, & \text{else.} \end{cases}$$

By construction,  $A$  is symmetric and we have  $\sum_{L \in \mathcal{T}} a_{K,L} = 0$  for any  $K \in \mathcal{T}$ . Hence, it is an easy task to conclude that  $A$  is positive semi-definite w.r.t. the standard scalar product. The vector  $u^n$  can be given in a closed formula by

$$u^n = (M + \tau A + \tau M\psi_\varepsilon)^{-1}M(u^{n-1} + g(u^{n-1})\Delta_n W). \quad (9)$$

Due to the fact that  $\psi_\varepsilon$  is non-linear and given by a case distinction and  $M + \tau A$  is not a diagonal matrix, we cannot calculate  $(M + \tau A + \tau M\psi_\varepsilon)^{-1}$  on a computer exactly. To this end, let us divide the calculation of  $u^n$  into two steps:

Step 1. Let  $u^{n-1} \in \mathbb{R}^{\tilde{d}}$  be given. Then we want to find  $\hat{u}^n \in \mathbb{R}^{\tilde{d}}$  such that

$$M(\hat{u}^n - u^{n-1}) + \tau A\hat{u}^n = Mg(u^{n-1})\Delta_n W.$$

Therefore  $\hat{u}^n$  is given by

$$\hat{u}^n := (M + \tau A)^{-1} M(u^{n-1} + g(u^{n-1}) \Delta_n W) \quad (10)$$

Step 2: For  $\hat{u}^n$  given by (10), we now want to find  $u^n$  satisfying

$$(M + \tau A)u^n + \tau M\psi_\varepsilon(u^n) = (M + \tau A)\hat{u}^n$$

and therefore  $u^n$  is given by

$$u^n + (M + \tau A)^{-1} \tau M\psi_\varepsilon(u^n) = \hat{u}^n. \quad (11)$$

If  $u^{n-1}$  is the solution of the FVS after  $n-1$  time steps,  $u^n$  is the solution of the FVS after  $n$  time steps. But due to the fact that  $\psi_\varepsilon$  is non-linear and defined by a case distinction and the fact that  $M + \tau A$  is not a diagonal matrix, we cannot give a closed formula for  $u^n$  which can be calculated by the computer properly. To this end, we want to cancel out the term  $\tau A$  in equation (11) and solve equation

$$\tilde{u}^n + \tau\psi_\varepsilon(\tilde{u}^n) = \hat{u}^n \quad (12)$$

for  $\tilde{u}^n \in \mathbb{R}^{\tilde{d}}$  instead. Equation (12) is vector-valued and since  $\psi_\varepsilon$  acts on each component separately, we can rewrite (12) as

$$\tilde{u}_K^n + \tau\psi_\varepsilon(\tilde{u}_K^n) = \hat{u}_K^n \text{ for each } K \in \mathcal{T}. \quad (13)$$

Now, since  $\psi_\varepsilon$  is monotone,  $I + \tau\psi_\varepsilon$  is strictly monotone and therefore invertible. Even though  $\psi_\varepsilon$  is non-linear and given by a case distinction, the unique solution of (13) on each control volume  $K \in \mathcal{T}$  is negative if and only if the right-hand side is negative, the solution is in  $[0, 1]$  if and only if the right-hand side is in  $[0, 1]$  and the solution is greater than 1 if and only if the right-hand side is greater than 1. Therefore, the solution of (13) is given by

$$\tilde{u}_K^n = (I + \tau\psi_\varepsilon)^{-1}(\hat{u}_K^n) \text{ for each } K \in \mathcal{T}, \quad (14)$$

where  $(I + \tau\psi_\varepsilon)^{-1}$  is given by

$$(I + \tau\psi_\varepsilon)^{-1}(r) = \begin{cases} \frac{\varepsilon r}{\varepsilon + \tau}, & r < 0 \\ r, & 0 \leq r \leq 1 \\ \frac{\varepsilon r + \tau}{\varepsilon + \tau}, & r > 1. \end{cases}$$

Hence,  $\tilde{u}_K^n$  is given by

$$\tilde{u}_K^n = \begin{cases} \frac{\varepsilon \hat{u}_K^n}{\varepsilon + \tau}, & \hat{u}_K^n < 0 \\ \hat{u}_K^n, & 0 \leq \hat{u}_K^n \leq 1 \\ \frac{\varepsilon \hat{u}_K^n + \tau}{\varepsilon + \tau}, & \hat{u}_K^n > 1. \end{cases}$$

This motivates the following definition:

**Definition 2.1.** Let  $n \in \{1, \dots, N\}$  and  $u_0 \in \mathbb{R}^{\tilde{d}}$  be given. Then,  $\tilde{u}^n = (\tilde{u}_K^n)_{K \in \mathcal{T}} \in \mathbb{R}^{\tilde{d}}$  defined by the recursion formula  $\tilde{u}^0 = u^0$ ,

$$\tilde{u}^n = (I + \tau\psi_\varepsilon)^{-1}(M + \tau A)^{-1}M(\tilde{u}^{n-1} + g(\tilde{u}^{n-1})\Delta_n W), \quad n \in \{1, \dots, N\}$$

is called the solution of the splitting method with initial datum  $u^0$ .

The upcoming theorem provides an error estimate between the solution of the FVS and the solution of the splitting method given the same initial datum  $u^0$ :

**Theorem 2.2.** Let  $u^0 \in \mathbb{R}^{\tilde{d}}$ ,  $\varepsilon > 0$  and  $N \in \mathbb{N}$  be given and  $u^n$  the solution of the FVS and  $\tilde{u}^n$  the solution of the splitting method, both with respect to  $u^0$ . Then there exists  $C > 0$  such that

$$\sup_{n \in \{1, \dots, N\}} \mathbb{E} \left[ \max_{K \in \mathcal{T}} |u_K^n - \tilde{u}_K^n| \right] \leq C \frac{\tau}{\varepsilon m_{\min}},$$

where  $m_{\min} := \inf_{K \in \mathcal{T}} m_K$ .

*Proof.* Let us set  $\tilde{A} := M^{-1}A$ . Then we have

$$(M + \tau A + \tau M\psi_\varepsilon)^{-1}M = (I + \tau \tilde{A} + \tau\psi_\varepsilon)^{-1} = (I + \tau(\tilde{A} + \psi_\varepsilon))^{-1}$$

and

$$(I + \tau\psi_\varepsilon)^{-1}(M + \tau A)^{-1}M = (I + \tau\psi_\varepsilon)^{-1}(I + \tau\tilde{A})^{-1}.$$

For  $B : \mathbb{R}^{\tilde{d}} \rightarrow \mathbb{R}^{\tilde{d}}$  we set  $\|B\|_2 := \sup_{x \neq y} \frac{|B(x) - B(y)|_2}{|x - y|_2}$ , where  $|\cdot|_2$  denotes the euclidian norm in  $\mathbb{R}^{\tilde{d}}$ . Then there exists  $C_1 = C_1(\xi) > 0$  such that

$$\|\tilde{A}\|_2 \leq \|M^{-1}\|_2 \|A\|_2 \leq \frac{C_1}{m_{\min}}.$$

First, we want to prove the theorem in the case where  $M$  is of the form  $M = m_{\min}I$ . Then  $\tilde{A} = m_{\min}^{-1}A$  and therefore  $\tilde{A}$  is positive semi-definite w.r.t. the standard scalar product and therefore monotone as a function from  $\mathbb{R}^{\tilde{d}}$  to  $\mathbb{R}^{\tilde{d}}$ . Since  $\psi_\varepsilon$  is monotone, we also have that  $\tilde{A} + \psi_\varepsilon$  is monotone and therefore

$$\begin{aligned} \|(I + \tau\tilde{A})^{-1}\|_2 &\leq 1, \\ \|(I + \tau\psi_\varepsilon)^{-1}\|_2 &\leq 1, \\ \|(I + \tau(\tilde{A} + \psi_\varepsilon))^{-1}\|_2 &\leq 1. \end{aligned} \tag{15}$$

Let us denote the abbreviations

$$\begin{aligned} S_\tau &:= (I + \tau(\tilde{A} + \psi_\varepsilon))^{-1}, \\ T_\tau &:= (I + \tau\psi_\varepsilon)^{-1}(I + \tau\tilde{A})^{-1}, \\ e_n &:= u^n - \tilde{u}^n, \\ w_{n-1} &:= u^{n-1} + g(u^{n-1})\Delta_n W, \\ h_{n-1} &:= (g(u^{n-1}) - g(\tilde{u}^{n-1}))\Delta_n W. \end{aligned}$$

Then we have

$$\begin{aligned} u^n &= S_\tau(w_{n-1}), \\ \tilde{u}^n &= T_\tau(\tilde{u}^{n-1} + g(\tilde{u}^{n-1})\Delta_n W) = T_\tau(w_{n-1} - e_{n-1} - h_{n-1}). \end{aligned}$$

Hence

$$\begin{aligned} e_n &= u^n - \tilde{u}^n = S_\tau(w_{n-1}) - T_\tau(w_{n-1} - e_{n-1} - h_{n-1}) \\ &= S_\tau(w_{n-1}) - T_\tau(w_{n-1}) + T_\tau(w_{n-1}) - T_\tau(w_{n-1} - e_{n-1} - h_{n-1}). \end{aligned}$$

Thanks to the inequality  $(x + y)^2 \leq (1 + \frac{1}{\tau})x^2 + (1 + \tau)y^2$ , we obtain

$$\begin{aligned} \mathbb{E} [|e_n|_2^2] &\leq (1 + \frac{1}{\tau})\mathbb{E} [|S_\tau - T_\tau|(w_{n-1})|_2^2] \\ &\quad + (1 + \tau)\mathbb{E} [|T_\tau(w_{n-1}) - T_\tau(w_{n-1} - e_{n-1} - h_{n-1})|_2^2] \\ &\leq (1 + \frac{1}{\tau})\|S_\tau - T_\tau\|_2^2\mathbb{E} [|w_{n-1}|_2^2] \\ &\quad + (1 + \tau)\|T_\tau\|_2^2\mathbb{E} [|e_{n-1} + h_{n-1}|_2^2]. \end{aligned}$$

Since

$$S_\tau - T_\tau = \tau^2(I + \tau\psi_\varepsilon)^{-1}(I + \tau\tilde{A})^{-1}\tilde{A}\psi_\varepsilon(I + \tau(\tilde{A} + \psi_\varepsilon))^{-1},$$

we have

$$\begin{aligned} \|S_\tau - T_\tau\|_2 &\leq \tau^2\|(I + \tau\psi_\varepsilon)^{-1}\|_2\|(I + \tau\tilde{A})^{-1}\|_2\|\tilde{A}\psi_\varepsilon\|_2\|(I + \tau(\tilde{A} + \psi_\varepsilon))^{-1}\|_2 \\ &\leq \tau^2\|\tilde{A}\psi_\varepsilon\|_2 \leq \frac{\tau^2}{\varepsilon}\|\tilde{A}\|_2. \end{aligned} \tag{16}$$

Moreover, there exists  $C_2 > 0$  such that  $\sup_{N \in \mathbb{N}} \sup_{n \in \{0, \dots, N\}} \mathbb{E} [|u^{n-1}|_2^2] \leq C_1$  and therefore we get

$$\begin{aligned} \mathbb{E} [|w_{n-1}|_2^2] &= \mathbb{E} [|u^{n-1}|_2^2 + 2u^{n-1} \cdot g(u^{n-1})\Delta_n W + |g(u^{n-1})\Delta_n W|_2^2] \\ &= \mathbb{E} [|u^{n-1}|_2^2 + |g(u^{n-1})|_2^2|\Delta_n W|^2] \\ &= \mathbb{E} [|u^{n-1}|_2^2] + \tau\mathbb{E} [|g(u^{n-1})|_2^2] \\ &\leq (1 + L_g^2\tau)\mathbb{E} [|u^{n-1}|_2^2] \\ &\leq (1 + L_g^2T)C_2 \end{aligned} \tag{17}$$

and

$$\begin{aligned}
\mathbb{E} [|e_{n-1} + h_{n-1}|_2^2] &= \mathbb{E} [|e_{n-1}|_2^2 + 2e_{n-1} \cdot h_{n-1} + |h_{n-1}|_2^2] \\
&= \mathbb{E} [|e_{n-1}|_2^2 + |g(u^{n-1}) - g(\tilde{u}^{n-1})|_2^2 |\Delta_n W|^2] \\
&= \mathbb{E} [|e_{n-1}|_2^2] + \tau \mathbb{E} [|g(u^{n-1}) - g(\tilde{u}^{n-1})|_2^2] \\
&\leq (1 + L_g^2 \tau) \mathbb{E} [|e_{n-1}|_2^2].
\end{aligned} \tag{18}$$

Thanks to (15) to (18) we obtain

$$\begin{aligned}
\mathbb{E} [|e_n|_2^2] &\leq (1 + \frac{1}{\tau}) \frac{\tau^4}{\varepsilon^2} \|\tilde{A}\|_2^2 (1 + L_g^2 T) C_2 \\
&\quad + (1 + \tau)(1 + L_g^2 \tau) \mathbb{E} [|e_{n-1}|_2^2] \\
&= \mathbb{E} [|e_{n-1}|_2^2] + (1 + \frac{1}{\tau}) \frac{\tau^4}{\varepsilon^2} \|\tilde{A}\|_2^2 (1 + L_g^2 T) C_2 \\
&\quad + \tau(1 + L_g^2 + L_g^2 \tau) \mathbb{E} [|e_{n-1}|_2^2] \\
&\leq \mathbb{E} [|e_{n-1}|_2^2] + \frac{(T+1)\tau^3}{\varepsilon^2} \|\tilde{A}\|_2^2 (1 + L_g^2 T) C_2 \\
&\quad + \tau(1 + L_g^2 + L_g^2 T) \mathbb{E} [|e_{n-1}|_2^2]
\end{aligned}$$

Subtracting  $\mathbb{E} [|e_{n-1}|_2^2]$ , replacing  $n$  by  $k$  and summing over  $k = 1, \dots, n$  yields

$$\begin{aligned}
\mathbb{E} [|e_n|_2^2] &\leq \frac{T(T+1)\tau^2}{\varepsilon^2} \|\tilde{A}\|_2^2 (1 + L_g^2 T) C_2 \\
&\quad + \tau(1 + L_g^2 + L_g^2 T) \sum_{k=1}^n \mathbb{E} [|e_{k-1}|_2^2]
\end{aligned}$$

From Gronwall's lemma we obtain a constant  $C_3 > 0$  such that

$$\sup_{n \in \{1, \dots, N\}} \mathbb{E} [|e_n|_2^2] \leq C_3 \|\tilde{A}\|_2^2 \frac{\tau^2}{\varepsilon^2} \leq C_3 C_1 \frac{\tau^2}{\varepsilon^2 m_{\min}^2}.$$

Hence we get

$$\sup_{n \in \{1, \dots, N\}} \mathbb{E} \left[ \sup_{K \in \mathcal{T}} |u_K^n - \tilde{u}_K^n| \right] \leq \left( \sup_{n \in \{1, \dots, N\}} \mathbb{E} [|e_n|_2^2] \right)^{\frac{1}{2}} \leq (C_3 C_1)^{\frac{1}{2}} \frac{\tau}{\varepsilon m_{\min}}.$$

In the general case where  $M$  is no longer necessarily of the form  $M = m_{\min} I$ ,  $\tilde{A}$  is no longer symmetric and therefore not positive semi-definite w.r.t. the

euclidian scalar product in general. Nevertheless, defining the scalar product  $\langle x, y \rangle_M := x^T M y$  for  $x, y \in \mathbb{R}^{\tilde{d}}$  we have

$$\langle x, \tilde{A}x \rangle_M = x^T Ax \geq 0$$

for any  $x \in \mathbb{R}^{\tilde{d}}$ . Hence,  $\tilde{A}$  is positive semi-definite w.r.t. the scalar product  $\langle \cdot, \cdot \rangle_M$  and we may repeat all previous arguments by replacing the euclidian scalar product with the scalar product  $\langle \cdot, \cdot \rangle_M$ . Since we have

$$m_{\min} |\cdot|_2 \leq |\cdot|_M \leq m_{\max} |\cdot|_2,$$

where  $m_{\max} = \sup_{K \in \mathcal{T}} m_K$  and  $|x|_M = \langle x, x \rangle_M$ , we get

$$\sup_{N \in \mathbb{N}} \sup_{n \in \{0, \dots, N\}} \mathbb{E} [|u^{n-1}|_M^2] \leq m_{\max}^2 \sup_{N \in \mathbb{N}} \sup_{n \in \{0, \dots, N\}} \mathbb{E} [|u^{n-1}|_2^2] \leq m_{\max}^2 C_1.$$

Since there exists a constant  $C_4 > 0$  such that  $m_{\max}/m_{\min} \leq C_4 \text{reg}(\mathcal{T})$ , there exists a constant  $C = C(\text{reg}(\mathcal{T})) > 0$  such that

$$\begin{aligned} \sup_{n \in \{1, \dots, N\}} \mathbb{E} \left[ \sup_{K \in \mathcal{T}} |u_K^n - \tilde{u}_K^n| \right] &\leq \left( \sup_{n \in \{1, \dots, N\}} \mathbb{E} [|e_n|_2^2] \right)^{\frac{1}{2}} \\ &\leq \left( \frac{1}{m_{\min}^2} \sup_{n \in \{1, \dots, N\}} \mathbb{E} [|e_n|_2^2] \right)^{\frac{1}{2}} \leq \left( \frac{m_{\max}^2}{m_{\min}^2} C_3 C_1 \right)^{\frac{1}{2}} \frac{\tau}{\varepsilon m_{\min}} \\ &= \frac{m_{\max}}{m_{\min}} (C_3 C_1)^{\frac{1}{2}} \frac{\tau}{\varepsilon m_{\min}} \\ &\leq C \frac{\tau}{\varepsilon m_{\min}}. \end{aligned}$$

□

The following lemma states some more properties of the matrix  $(M + \tau A)^{-1}M$ . If  $Z$  is a vector or a matrix, we denote  $Z \geq 0$  if and only if all components of  $Z$  are non-negative. Similarly, we denote  $Z \leq 0$  if and only if  $-Z \geq 0$ .

**Lemma 2.3.** *Let  $x \in \mathbb{R}^{\tilde{d}}$  with  $x \geq 0$ . Then  $(M + \tau A)^{-1}Mx \geq 0$ .*

*Proof.* Since  $A$  is symmetric and positive semi-definite with non-positive off-diagonal components,  $M + \tau A$  is symmetric and positive definite with non-positive off-diagonal components. Hence,  $M + \tau A$  is a Stieltjes matrix and therefore  $(M + \tau A)^{-1} \geq 0$ . Especially, if  $x \in \mathbb{R}^{\tilde{d}}$  with  $x \geq 0$ , then  $(M + \tau A)^{-1}x \geq 0$ . □

Now we show that if pathwise the values of all components of the solution of the splitting method after  $n - 1$  time steps  $\tilde{u}^{n-1}$  are below the threshold 0 (or above the threshold 1, respectively), then this will be the case for all subsequent time steps. In the following, we will denote by  $\mathbf{1} \in \mathbb{R}^{\tilde{d}}$  the vector whose components are all equal to 1.

**Corollary 2.4.** *Let  $\tilde{u}^{n-1} \in \mathbb{R}^{\tilde{d}}$  such that  $\tilde{u}^{n-1} \leq 0$  or  $\tilde{u}^{n-1} - \mathbf{1} \geq 0$ , respectively. Moreover, let  $\tilde{u}^n \in \mathbb{R}^{\tilde{d}}$  be the solution of the splitting method. Then  $\tilde{u}^n \leq 0$  or  $\tilde{u}^n - \mathbf{1} \geq 0$ , respectively.*

*Proof.* Let  $\tilde{u}^{n-1} \in \mathbb{R}^{\tilde{d}}$  with  $\tilde{u}^{n-1} \leq 0$  or  $\tilde{u}^{n-1} - \mathbf{1} \geq 0$ , respectively. Then, since  $\text{supp}(g) \subset [0, 1]$  we have  $g(\tilde{u}^{n-1}) = 0 \in \mathbb{R}^{\tilde{d}}$  and therefore we obtain

$$\begin{aligned}\tilde{u}^n &= (I + \tau\psi_\varepsilon)^{-1}(M + \tau A)^{-1}M(\tilde{u}^{n-1} + g(\tilde{u}^{n-1})\Delta_n W) \\ &= (I + \tau\psi_\varepsilon)^{-1}(M + \tau A)^{-1}M(\tilde{u}^{n-1}).\end{aligned}$$

Now, if  $\tilde{u}^{n-1} \leq 0$  Lemma 2.3 yields  $(M + \tau A)^{-1}M(\tilde{u}^{n-1}) \leq 0$  and therefore  $\tilde{u}^n \leq 0$ . Since  $A\mathbf{1} = 0$  we have

$$\mathbf{1} = (M + \tau A)^{-1}M\mathbf{1}.$$

Therefore, if  $\tilde{u}^{n-1} - \mathbf{1} \geq 0$  Lemma 2.3 yields

$$(M + \tau A)^{-1}M(\tilde{u}^{n-1}) - \mathbf{1} = (M + \tau A)^{-1}M(\tilde{u}^{n-1} - \mathbf{1}) \geq 0.$$

Hence, since  $(I + \tau\psi_\varepsilon)^{-1}$  is non-decreasing and  $(I + \tau\psi_\varepsilon)^{-1}\mathbf{1} = \mathbf{1}$ , we obtain  $\tilde{u}^n - \mathbf{1} \geq 0$ .  $\square$

### 3 Numerical experiments

All upcoming experiments were performed on an Apple M2 Pro with 16GB RAM in Python. Therein we use  $\Lambda = (-1, 1)^2$ ,  $T = 1$  and

$$u_0(x, y) = \left( \frac{1}{16}x^4 + \frac{1}{4}x^3 - \frac{1}{8}x^2 - \frac{3}{4}x + \frac{9}{16} \right) \left( \frac{3}{32}y^4 - \frac{1}{4}y^3 - \frac{3}{16}y^2 + \frac{3}{4}y + \frac{19}{32} \right)$$

as a non-symmetric and non-trivial initial value satisfying the homogeneous Neumann boundary condition and  $0 \leq u_0(x, y) \leq 1$  for all  $x, y \in [-1, 1]$ . We set  $u^0 := u_h^0 := (u_K^0)_{K \in \mathcal{T}}$  as in Section 1. Unless otherwise specified, for the noise term  $g$  we use

$$g(x) = ax(1 - x)\mathbf{1}_{[0,1]}(x), \quad x \in \mathbb{R}$$

for different parameters  $a > 0$ . In order to compute the expectation we use the classical Monte Carlo method with  $N_p$  realizations. We will divide the domain  $\Lambda$  into subsquares with equal size which are our control volumes. The parameters  $L$  or  $L_{max}$  will denote the number of squares in each spatial direction, i.e., the total number of subsquares used for the spatial discretization is  $L^2$  or  $L_{max}^2$  and the 2-d Lebesgue measure of those subsquares is  $4/L^2$  or  $4/L_{max}^2$ , respectively. Therefore, we have  $h = \sqrt{8}/L$  or  $h = \sqrt{8}/L_{max}$ , respectively. In all upcoming experiments, the splitting method introduced in Section 2 is used in order to compute approximate solutions of the Allen-Cahn equation (1). This choice of parameters does not refer to theoretical results but only to the experiments that substantiate the results.

### 3.1 Pathwise properties

#### 3.1.1 General behaviour of the splitting method

At first, let us explain the genereal behaviour of the solution of the splitting method based on an example. Set  $a = 10$  and  $L = 2$ . Then  $\mathcal{T} = \{K_0, K_1, K_2, K_3\}$ , where  $K_0 = (-1, 0)^2$ ,  $K_1 = (-1, 0) \times (0, 1)$ ,  $K_2 = (0, 1) \times (-1, 0)$  and  $K_3 = (0, 1)^2$ . Moreover, for a fixed path of the Brownian motion let us say we approximately have

$$\begin{aligned}\Delta_1 W &= W_{\frac{1}{4}} - W_0 = -0.6046086559049673, \\ \Delta_2 W &= W_{\frac{1}{2}} - W_{\frac{1}{4}} = 0.6937104821525855, \\ \Delta_3 W &= W_{\frac{3}{4}} - W_{\frac{1}{2}} = -1.1713571186231886, \\ \Delta_4 W &= W_1 - W_{\frac{3}{4}} = 0.24606633895637547.\end{aligned}$$

For the approximate initial value we have

$$u^0 = (u_0^0, u_1^0, u_2^0, u_3^0) = (0.20088542, 0.05244792, 0.72953125, 0.19046875).$$

The solutions of the splitting method for  $N = 2$ ,  $n \in \{1, 2\}$  iterations and  $\varepsilon = (1/10) \cdot (T/N)^3$  are displayed in Table 1. We compare these values to the values of the FVS of the SHE, i.e., in the case  $\psi_\varepsilon \equiv 0$ , which are displayed in Table 2.

Table 1: Solutions of the splitting method for  $N = 2$

n	$\tilde{u}^n$
1	( 0.39495382, 0.24383317, 0.64814013, 0.38692093)
2	( -0.23254276, -0.21628772, -0.21627557, -0.23198247)

Table 2: Solutions of SHE for  $N = 2$ 

n	$\hat{u}^n$
1	( 0.39495382, 0.24383317, 0.64814013, 0.38692093)
2	( -1.69747036, -1.57881501, -1.57872628, -1.69338044)

Since the values of  $\tilde{u}^1$  on each control volume are inside  $[0, 1]$ , the term  $\psi_\varepsilon$  did not play any role in the calculation of  $\tilde{u}^1$ . Hence,  $\tilde{u}^1$  coincides with  $\hat{u}^1$ , the solution of the FVS of the SHE after  $n = 1$  time steps. Observing the values of  $\tilde{u}^2$  we already see that the splitting method is not structure-preserving, i.e., the values of the solution of the splitting method are not pathwise in  $[0, 1]$ . Actually, this is not a surprise since we work with the Yosida approximation  $\psi_\varepsilon$  and not the sub-differential  $\partial I_{[0,1]}$  itself. Moreover, since the values of  $\tilde{u}^2$  are not inside  $[0, 1]$ , we obtain  $\tilde{u}^2 \neq \hat{u}^2$  and the values of  $\tilde{u}^2$  are much closer to the threshold 0 than the values of  $\hat{u}^2$ .

For  $N = 4$  we obtain Table 3 for the splitting method.

 Table 3: Solutions of the splitting method for  $N = 4$ 

n	$\tilde{u}^n$
1	( -0.13385192, -0.07727270, -0.10617873, -0.13010620)
2	( -0.02478902, -0.01854758, -0.02242615, -0.02428642)
3	( -0.00476855, -0.00406696, -0.00458739, -0.00470111)
4	( -0.00093698, -0.00085652, -0.00092635, -0.00092793)

Here we see that the values of  $\tilde{u}^1$  on each control volume are less than 0. Thanks to Corollary 2.4 the values of the components of  $\tilde{u}^2, \tilde{u}^3$  and  $\tilde{u}^4$  should be less or equal 0, which is actually the case. Now, the task of  $\psi_\varepsilon$  is to push the values below 0 (above 1, respectively) in the direction of 0 (of 1, respectively).

### 3.1.2 Constant solutions

In this section we tackle the question in which cases solutions of the FVS and the splitting method are constant in space or even constant in space-time. It is well known that if the initial value is constant in space then the solution of the Allen-Cahn equation is constant in space.

**Theorem 3.1.** *Let  $u^0 \in \mathbb{R}^d$  be pathwise constant, i.e., for each fixed  $\omega \in \Omega$  there exists  $c \in [0, 1]$  such that  $u_K^0(\omega) = u_L^0(\omega) = c$  for each  $K, L \in \mathcal{T}$ . Moreover, for  $N \in \mathbb{N}$  let  $u^n = (u_K^n)_{K \in \mathcal{T}}$  be the solution of the FVS after*

$n$  time steps and  $(\tilde{u}_K^n)_{K \in \mathcal{T}}$  the solution of the splitting method after  $n$  time steps. Then we obtain pathwise

$$\tilde{u}_K^n = u_K^n = u_L^n = \tilde{u}_L^n \text{ for all } n \in \{1, \dots, N\} \text{ and } K, L \in \mathcal{T}.$$

*Proof.* By induction, we only need to proof the assertions for  $n = 1$ . The vector  $u^1$  is given by the formula

$$\begin{aligned} u^1 &= (M + \tau A + \tau M \psi_\varepsilon)^{-1} M(u^0 + g(u^0) \Delta_1 W) \\ &= (I + \tau M^{-1} A + \tau \psi_\varepsilon)^{-1} (u^0 + g(u^0) \Delta_1 W). \end{aligned}$$

We set  $\bar{u}^1 := (I + \tau \psi_\varepsilon)^{-1} (u^0 + g(u^0) \Delta_1 W)$ . Let us remark that

$$\begin{aligned} (u^0 + g(u^0) \Delta_1 W)_K &= u_K^0 + g(u_K^0) \Delta_1 W \\ u_L^0 + g(u_L^0) \Delta_1 W &= (u^0 + g(u^0) \Delta_1 W)_L \end{aligned}$$

for all  $K, L \in \mathcal{T}$ . Then we have

$$\begin{aligned} \bar{u}^1 &:= (I + \tau \psi_\varepsilon)^{-1} (u^0 + g(u^0) \Delta_1 W) \\ &\Leftrightarrow (I + \tau \psi_\varepsilon)(\bar{u}^1) = u^0 + g(u^0) \Delta_1 W \\ &\Leftrightarrow ((I + \tau \psi_\varepsilon)(\bar{u}^1))_K = (u^0 + g(u^0) \Delta_1 W)_K \text{ for all } K \in \mathcal{T} \quad (19) \\ &\Leftrightarrow \bar{u}_K^1 + \tau \psi_\varepsilon(\bar{u}_K^1) = u_K^0 + g(u_K^0) \Delta_1 W \text{ for all } K \in \mathcal{T} \\ &\Leftrightarrow \bar{u}_K^1 = (I + \tau \psi_\varepsilon)^{-1} (u_K^0 + g(u_K^0) \Delta_1 W) \text{ for all } K \in \mathcal{T}. \end{aligned}$$

Hence,  $\bar{u}_K^1 = \bar{u}_L^1$  for all  $K, L \in \mathcal{T}$ . Moreover, since  $A\mathbf{1} = 0$  we get  $A(\bar{u}^1) = 0$ . Therefore

$$(I + \tau \psi_\varepsilon)(\bar{u}^1) = (I + \tau M^{-1} A + \tau \psi_\varepsilon)(\bar{u}^1)$$

and

$$\bar{u}^1 = (I + \tau M^{-1} A + \tau \psi_\varepsilon)^{-1} (u^0 + g(u^0) \Delta_1 W) = u^1.$$

For the solution of the splitting method we have

$$\tilde{u}^1 = (I + \tau \psi_\varepsilon)^{-1} (M + \tau A)^{-1} M(u^0 + g(u^0) \Delta_1 W).$$

Since all components of  $u^0 + g(u^0) \Delta_1 W$  are equal, the equality  $A\mathbf{1} = 0$  yields that

$$(M + \tau A)^{-1} M(u^0 + g(u^0) \Delta_1 W) = u^0 + g(u^0) \Delta_1 W.$$

Now, similar arguments as in (19) yield  $\tilde{u}_K^1 = \tilde{u}_L^1$  for all  $K, L \in \mathcal{T}$ .  $\square$

If  $c \in [0, 1]$  such that  $g(c) = 0$ , it is well known that  $u$  defined by  $u(t, x) = c$  for all  $t \in [0, T]$  and  $x \in \Lambda$  is a solution of the Allen-Cahn equation. The same applies to the solution of the FVS and the splitting method.

**Theorem 3.2.** *Let  $u^0 \in \mathbb{R}^{\tilde{d}}$  be pathwise constant, i.e., for each fixed  $\omega \in \Omega$  there exists  $c \in [0, 1]$  such that  $u_K^0(\omega) = u_L^0(\omega) = c$  for each  $K, L \in \mathcal{T}$  and let  $g(c) = 0$ . Moreover, for  $N \in \mathbb{N}$  let  $u^n = (u_K^n)_{K \in \mathcal{T}}$  be the solution of the FVS after  $n$  time steps and  $(\tilde{u}_K^n)_{K \in \mathcal{T}}$  the solution of the splitting method after  $n$  time steps. Then we obtain pathwise*

$$u_K^n = \tilde{u}_K^n = c \text{ for all } n \in \{1, \dots, N\} \text{ and } K, L \in \mathcal{T}.$$

*Proof.* By induction we only need to prove the assertion for  $n = 1$ . Repeating the arguments in the proof of Theorem 3.1 we have

$$u_K^1 = \tilde{u}_K^1 = (I + \tau \psi_\varepsilon)^{-1}(u_K^0) = (I + \tau \psi_\varepsilon)^{-1}(c) \text{ for all } K \in \mathcal{T}.$$

By definition of  $(I + \tau \psi_\varepsilon)^{-1}$ , we obtain  $u_K^1 = \tilde{u}_K^1 = c$  for all  $K \in \mathcal{T}$ .  $\square$

After a benchmark test of Theorem (3.1) and (3.2) our scheme is accurate.

### 3.2 Expected value of the solution

Since  $\int_{\Lambda} \Delta u(t) dx = \int_{\partial \Lambda} \nabla u(t) \cdot \mathbf{n} dS = 0$  for almost every  $t \in (0, T)$ , after integrating (3) over  $\Lambda$  and applying the expectation we obtain:

$$\int_{\Lambda} \mathbb{E}[u(t)] dx = \int_{\Lambda} \mathbb{E}[u_0] dx - \int_{\Lambda} \int_0^t \mathbb{E}[\psi(s)] ds dx$$

for  $\psi \in \partial I_{[0,1]}(u)$  almost everywhere in  $\Omega \times (0, T) \times \Lambda$ . Hence, the more the subdifferential must keep the solution above the threshold 0 or below the threshold 1, the greater the difference between  $\int_{\Lambda} \mathbb{E}[u(t)] dx$  and  $\int_{\Lambda} \mathbb{E}[u_0] dx$ . We may observe the same phenomenon in our numerical experiments: Let us denote by  $\tilde{u}_n^N = (\tilde{u}_{N,K}^n)_{K \in \mathcal{T}}$  the solution of the splitting method for  $N \in \mathbb{N}$

after  $n$  time steps. Moreover, let us denote by  $E_K(\tilde{u}_N^n) := \frac{1}{N_p} \sum_{k=1}^{N_p} \tilde{u}_{N,K}^n(\omega_k)$  the estimated approximation of the expectation of  $\tilde{u}_{N,K}^n$  via Monte-Carlo method for  $N_p$  paths  $\omega_1, \dots, \omega_{N_p} \in \Omega$  and  $K \in \mathcal{T}$ . Then,  $E(\tilde{u}_N^n) := \frac{1}{|\mathcal{T}|} \sum_{K \in \mathcal{T}} E_K(\tilde{u}_N^n)$

denotes an approximation of  $\frac{1}{\Lambda} \int_{\Lambda} \mathbb{E}[u(t_n)] dx$  via splitting method. Now we choose  $\mathcal{T} = \{K_0, \dots, K_{L^2-1}\}$ , where  $K_n = (-1 + \frac{2k}{L}, -1 + \frac{2k+2}{L}) \times (-1 + \frac{2m}{L}, -1 + \frac{2m+2}{L})$  and  $m, k \in \{0, \dots, L-1\}$  such that  $n = Lk + m$ . We choose  $L = 5$ ,  $N = 2048$ ,  $N_p = 3000$  and  $a \in \{1, 3, 10, 40\}$ . Then we have  $E(u^0) = 0.29333333$  and

Table 4: Mean of  $\tilde{u}_n^N$  for  $a \in \{1, 3, 10, 40\}$ ,  $n = 2$  and  $N = 2048$

a	$\tilde{u}_N^n$	$ E(u^0) - E(\tilde{u}_N^n) $
1	0.29466193	0.0013286
3	0.32526468	0.03193135
10	0.37757956	0.08424623
40	0.45968785	0.16635452

Table 5: Mean of  $\tilde{u}_n^N$  for  $a \in \{1, 3, 10, 40\}$ ,  $n = 64$  and  $N = 2048$

a	$\tilde{u}_N^n$	$ E(u^0) - E(\tilde{u}_N^n) $
1	0.29380818	0.00047485
3	0.30069061	0.00735728
10	0.30783147	0.01449814
40	0.37980240	0.08646907

Table 6: Mean of  $\tilde{u}_n^N$  for  $a \in \{1, 3, 10, 40\}$ ,  $n = 2048$  and  $N = 2048$

a	$\tilde{u}_N^n$	$ E(u^0) - E(\tilde{u}_N^n) $
1	0.29387679	0.00054346
3	0.30050788	0.00717455
10	0.27745881	0.01587452
40	0.30688916	0.01355583

### 3.3 Numerical error estimates

Nummer der simulierten Paths, L=...

- $L_{max}$  in Musterlösung  $u_{max}$  und in Approximationen gleich, Focus auf den zeitlichen Fehler, 9000 Paths
- $L_{max}$  in Musterlösung  $u_{max}$  und in  $L$  in Approximationen verschieden, Focus auf den räumlichen Fehler bei weniger Pfaden
- Die Rolle der Lipschitzkonstanten  $C_g$  bei der Fehlerabschätzung
- Numerical error estimates im deterministischen Fall, d.h.  $dW$  wird durch  $dt$  ersetzt; auch deterministisch ist das Verfahren nicht structure-preserving

In this section we provide estimates of the error between  $\tilde{u}_{L_{max}, N_{max}}^{N_{max}}$  and  $\tilde{u}_{L, N}^N$ . More precisely, we calculate the quantity

$$E(L, L_{max}, N, N_{max}, N_p) := \frac{1}{N_p} \sum_{i=1}^{N_p} \|\tilde{u}_{L_{max}, N_{max}}^{N_{max}}(\omega_i) - \tilde{u}_{L, N}^N(\omega_i)\|_{L^2(\Lambda)}^2$$

for  $\omega_i \in \Omega$ ,  $i = 1, \dots, N_p$ , where  $\tilde{u}_{L,N}^N := \tilde{u}_{h,N}^N$  for  $h = \frac{\sqrt{8}}{L}$  and  $\tilde{u}_{L_{max},N_{max}}^{N_{max}} := \tilde{u}_{h_{max},N_{max}}^{N_{max}}$  for  $h_{max} = \frac{\sqrt{8}}{L_{max}}$ , respectively, are identified with its respective simple function on  $\Lambda$ . At first, we will focus on the case  $L = L_{max} = 4$ . Let us mention that the computational error does not change significantly for larger  $L$  here. In the following graphs we use  $N_p = 9000$ ,  $N_{max} = 40320$  and  $N \in N_1 = \{210, 280, 360, 504, 630, 840, 1008, 1260, 1680, 2520, 3360, 4032, 5040\}$ . The graphs are displayed in a log-log-scale. The blue dots determine the computational error and the orange line is a linear regression line. We will denote by  $m$  the slope of the orange graph, i.e.,  $E(L, L, N_{max}, N) \approx C\tau^m$  for some  $C > 0$ . From [SZ25] we know that  $m = 1$  for the stochastic heat equation, therefore we expect for  $a$  being small a computational order of convergence  $m$  close to 1, but for large  $a$  we might obtain a computational order of convergence  $m$  less than 1. In the following, we choose  $\varepsilon = \frac{1}{10}\tau^{0.4}$ . The order of computational order can be seen in table 7 and figures 2 and 3.

Table 7: Order of convergence for  $a \in \{1, 5, 30, 60\}$

a	m
1	1.05987278
5	1.01879060
30	0.22905177
60	0.14004819

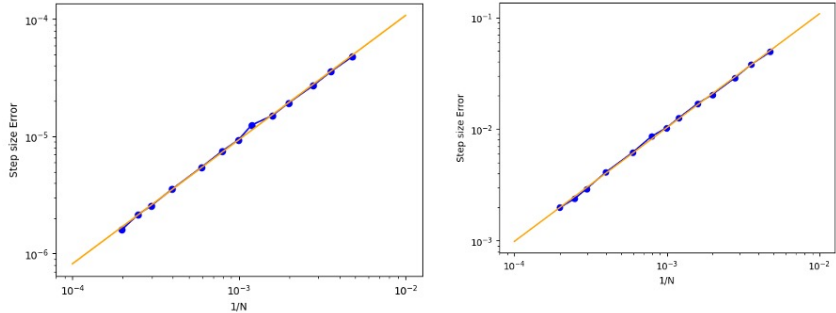


Figure 2: First graph: squared  $L^2$ -error with  $a = 1$ . Second graph: squared  $L^2$ -error with  $a = 5$ .

The very low computational order of convergence for  $a = 30, 60$  might be a result of the fact that the values for  $N$  and  $N_{max}$  are too low. Therefore, we repeat the experiment for  $a = 60$ ,  $N_p = 3000$ ,  $N_{max} = 403200$ ,  $N \in N_1 \cup N_2$ ,

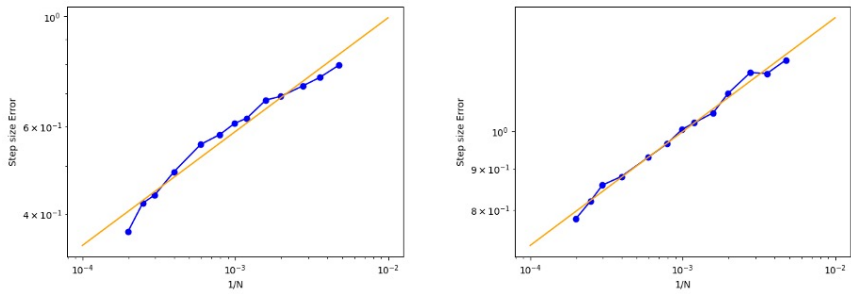


Figure 3: First graph: squared  $L^2$ -error with  $a = 30$ . Second graph: squared  $L^2$ -error with  $a = 60$ .

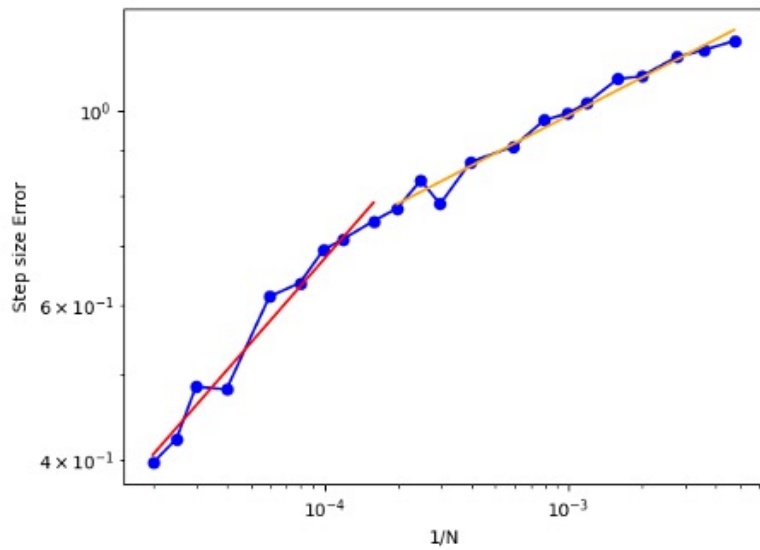


Figure 4: squared  $L^2$ -error with  $a = 60$  for  $N \in N_1 \cup N_2$ .

where  $N_2 = \{6300, 8400, 10080, 12600, 16800, 25200, 33600, 40320, 50400\}$ . The orange line determines the linear regression line for  $N \in N_1$  and the red line the linear regression for  $N \in N_2$ . For  $N \in N_1$  we obtain  $m = 0.14360763$ , as expected close to the previous result, and for  $N \in N_2$  we get  $m = 0.31759428$  (see figure 4). Hence, for large  $a$ , as  $N$  increases the computational order of convergence increases.

## References

- [ACQS20] R. Anton, D. Cohen and L. Quer-Sardanyons. A fully discrete approximation of the one-dimensional stochastic heat equation. *IMA J. Numer. Anal.*, 40(1):247–284, 2020.
- [BBNP14] Ł. Bañas, Z. Brzeźniak, M. Neklyudov and A. Prohl. *Stochastic ferromagnetism*, volume 58 of *De Gruyter Studies in Mathematics*. De Gruyter, Berlin, 2014. Analysis and numerics.
- [Bar76] V. Barbu. *Nonlinear Semigroups and Differential Equations in Banach Spaces*. Noordhoff, Leyden, 1976.
- [BBBLV17] C. Bauzet, E. Bonetti, G. Bonfanti, F. Lebon and G. Vallet: A global existence and uniqueness result for a stochastic Allen-Cahn equation with constraint. *Math. Methods Appl. Sci.* 40 (14) (2017) 5241–5261
- [BCC20] C. Bauzet, V. Castel, and J. Charrier. Existence and uniqueness result for an hyperbolic scalar conservation law with a stochastic force using a finite volume approximation. *J. Hyperbolic Differ. Equ.*, 17(2):213–294, 2020.
- [BCG162] C. Bauzet, J. Charrier and T. Gallouët. Convergence of flux-splitting finite volume schemes for hyperbolic scalar conservation laws with a multiplicative stochastic perturbation. *Math. Comp.*, 85(302):2777–2813, 2016.
- [BCG161] C. Bauzet, J. Charrier and T. Gallouët. Convergence of monotone finite volume schemes for hyperbolic scalar conservation laws with multiplicative noise. *Stoch. Partial Differ. Equ. Anal. Comput.*, 4(1):150–223, 2016.
- [BCG17] C. Bauzet, J. Charrier and T. Gallouët. Numerical approximation of stochastic conservation laws on bounded domains. *ESAIM Math. Model. Numer. Anal.*, 51(1):225–278, 2017.

[BHL21] D. Breit, M. Hofmanová and S. Loisel. Space-time approximation of stochastic  $p$ -Laplace-type systems. *SIAM J. Numer. Anal.*, 59(4):2218–2236, 2021.

[BNSZ22] C. Bauzet, F. Nabet, K. Schmitz and A. Zimmermann. Convergence of a finite-volume scheme for a heat equation with a multiplicative Lipschitz noise. *ESAIM Math. Model. Numer. Anal.*, 57(2):745–783, 2022.

[BNSZ23] C. Bauzet, F. Nabet, K. Schmitz and A. Zimmermann. Finite Volume Approximations for Non-linear Parabolic Problems with Stochastic Forcing. In *Finite Volumes for Complex Applications X—Volume 1, Elliptic and Parabolic Problems*, volume 432 of *Springer Proc. Math. Stat.*, pages 157–166. Springer, Cham, 2023.

[Bre73] H. Brézis *Opérateurs Maximaux Monotones et Semi-groupes de Contractions dans les Espaces de Hilbert*. Number 5 in North Holland Math. Studies, 1973.

[BSZ25] C. Bauzet, K. Schmitz and A. Zimmermann: On a finite-volume approximation of a diffusion-convection equation with a multiplicative stochastic force. *Stoch PDE: Anal Comp* (2025). <https://doi.org/10.1007/s40072-025-00379-8>

[BSVZ25] C. Bauzet, C. Sultan, G. Vallet and A. Zimmermann: Theoretical analysis of a finite-volume scheme for a stochastic Allen–Cahn problem with constraint. *Nonlinear Analysis*, Volume 259, 2025, 113812, <https://doi.org/10.1016/j.na.2025.113812>

[DP09] A. Debussche and J. Printems. Weak order for the discretization of the stochastic heat equation. *Math. Comp.*, 78(266):845–863, 2009.

[D14] J. Droniou. Finite volume schemes for diffusion equations: Introduction to and review of modern methods. *Mathematical Models and Methods in Applied Sciences*, 24(08):1575–1619, 2014.

[EGH00] R. Eymard, T. Gallouët and R. Herbin. Finite Volume Methods. *Handb. numer. anal.*, vii, 2000, pp. 713–1020.

[OPW20] M. Ondrejat, A. Prohl and N. Walkington. Numerical approximation of nonlinear SPDE’s. *Stoch. and Partial Differ. Equ.: Anal. Comput.*, 2022.

[SZ25] N. Sapountzoglou and A. Zimmermann: Convergence Rates for a Finite Volume Scheme of the Stochastic Heat Equation. *Computational*

Methods in Applied Mathematics (2025). <https://doi.org/10.1515/cmam-2024-0089>